

# Surface-Texture Evolution of Different Chemical-Vapor-Deposited Zinc Sulfide Flats Polished with Various Magnetorheological Fluids

## Introduction

Zinc sulfide (ZnS) is an infrared (IR) optical material widely used for applications such as IR windows, domes, and optical lenses.<sup>1</sup> It is industrially produced by the chemical-vapor-deposition (CVD) technique to reach a dense, milky yellow–orange color, with ~70% transmission in the mid-long-wave IR region.<sup>1</sup> Its inner structure consists of cone-like structures that grow larger as deposition takes place, up to a thickness of a few centimeters.<sup>2,3</sup> These cone-like structures manifest on the top of the deposited surface as “pebbles”<sup>2</sup> or “hillocks”<sup>4</sup> and are often called “alligator skin.”<sup>5</sup>

The importance of good surface finishing of an optical component is well understood. The lack of good finishing results in the scattering and absorption of light, leading to low optical performance.<sup>1,6</sup> Polishing out the pebble structure from a CVD ZnS substrate to a relatively smooth [ $<3$ -nm root mean square (rms)] surface is quite challenging, especially for an undestructive polishing process<sup>7</sup> (that leaves no plastic deformation and does not destroy the crystallographic array of the top finished layer), such as the magnetorheological finishing (MRF) technique.

MRF is a deterministic, sub-aperture polishing process that is capable of polishing flats, spheres, and aspheric shapes.<sup>8</sup> It uses a magnetorheological (MR) fluid composed of micron-size carbonyl iron (CI) powder, water, stabilizing additives, and abrasives (like ceria or nanodiamonds). When exposed to a magnetic field, the fluid stiffens as the CI particles align with the magnetic field, and functions as a polishing pad with a layer of nonmagnetic abrasive particles on the top layer. This fluid is kept at a relatively high pH (10 or higher) to suppress corrosion of the iron particles. By suppressing corrosion, a conventional MR fluid can last more than three weeks.

Kozhinova *et al.*<sup>2</sup> and Hallock *et al.*<sup>9</sup> demonstrated an improvement in surface artifacts on CVD ZnS and zinc selenide (ZnSe), respectively, during MRF by using acidic (pH ~4.5) MR fluids and soft CI particles; however, the MR fluids used in their work did not provide consistent and repeatable results. The two

main challenges they faced were (a) a material-removal-rate performance that varied among CVD ZnS substrates manufactured by different vendors (0.5 to 1.5  $\mu\text{m}/\text{min}$ ) and (b) rapid corrosion of the CI particles in the MR fluid.

There is no consensus of deposition parameters for CVD ZnS.<sup>4,10</sup> Different manufacturers select different deposition conditions (such as deposition temperature, pressure, and vapor velocity). Therefore, it is reasonable to assume that physical properties of the final product, such as color, average grain size, and crystallographic orientation volume fraction, are different among vendors and might lead to variations in polishing results among different parts during MRF.

In 2008 a novel zirconia sol-gel coating process to protect CI particles from corrosion was invented at the University of Rochester.<sup>11</sup> These coated particles were successfully mixed into a MR fluid at pH 8 to perform a MRF experiment on several optical substrates.<sup>12</sup> In 2013 (Ref. 13) we reported on a MRF experiment using MR fluids based on the same zirconia-coated CI (Zr-CI) particles at pH levels of 4, 5, and 6 as in Fig. 142.27. In that experiment we used single-crystal

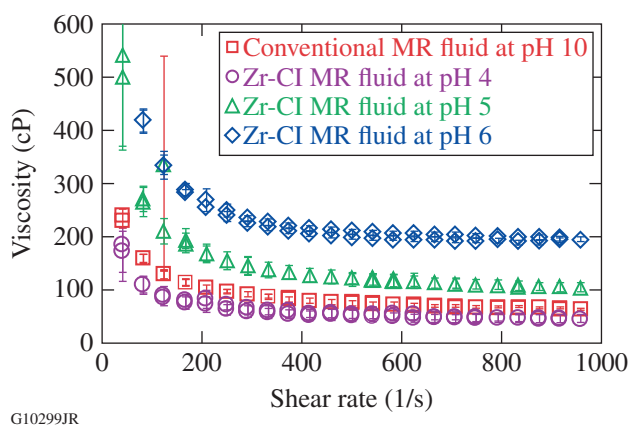


Figure 142.27 Viscosity versus shear-rate plot for conventional MR fluid at pH 10 (squares) and zirconia-coated-CI (Zr-CI) MR fluids at pH 4 (circles), pH 5 (triangles), and 6 pH (diamonds).

ZnS planes to investigate the role of material-removal-rate anisotropy of polycrystalline (pc) CVD ZnS during MRF. The results showed a relatively uniform removal rate ( $0.06 \mu\text{m}/\text{min}$ ) for single-crystal planes when using MR fluid at pH 4. The conclusions presented here predicted an improvement in surface artifacts (the emergence of pebbles on the surface) when using this type of fluid for MRF polishing of a CVD ZnS substrate.

Here the authors present the surface-texture evolution of several differently grown CVD ZnS substrates that were MRF polished with four MR fluids at pH levels of 10, 6, 5, and 4. The goal was twofold: to check (1) if a decrease in MR fluid pH improves the surface artifacts of a CVD ZnS surface during MRF polishing; and (2) if MR fluid pH is capable of dealing with part-to-part variations in the surface texture among CVD ZnS materials deposited by different vendors.

## Experimental

### 1. Polycrystalline CVD ZnS Substrates

Four CVD ZnS substrates were purchased from four different vendors: one is an elemental CVD ZnS substrate purchased from China; the other three are forward-looking-infrared (FLIR) CVD ZnS substrates purchased from China and the U.S. The difference between the two types is the chemical reaction of the precursor gases (for more information, refer to Refs. 1 and 6). We will refer to them as substrates A (FLIR, U.S.), B (FLIR, U.S.), C (FLIR, China), and D (elemental, China). Each sample measured 40 mm in diameter and 5 mm in thickness. The samples were pre-polished in-house on pitch with diamond abrasives (as described in Ref. 2) to a peak-to-valley (p-v) flatness of  $1\lambda$  to  $2\lambda$  and an areal roughness of less than 27-nm p-v and 2-nm rms.

### 2. X-Ray Diffraction

To determine the relative portion of crystallite orientations within the samples, an x-ray diffraction (XRD) analysis was performed using a general-purpose x-ray diffractometer (Philips X'Pert, MPD system). Cu  $K_{\alpha 1}$  radiation ( $\lambda_{\text{Cu}} = 1.5418 \text{ \AA}$ ) was used to produce an x-ray diffraction pattern in a  $2\theta$  angle range of

$10^\circ$  to  $70^\circ$  with step intervals of  $2\theta = 0.03^\circ$ . The diffraction data were analyzed using X'Pert High Score software. The reference database for cubic ZnS was taken from the Joint Committee for Powder Diffraction Standards (JCPDS) filed by the International Centre for Diffraction Data, Newtown Square, PA. We used JCPDS files 65-0309, 65-5476, and 65-1691.

### 3. MRF Spotting Experiment

MRF spotting experiments were performed on a research platform referred to as the "spot-taking machine" (STM). It has features similar to a conventional MRF machine; however, it is free to move only in the vertical  $z$  direction. Consequently, it is capable of performing only single spots on the surface. The MR fluids used here were a conventional diamond fluid (D11) at pH 10, purchased from QED Technologies<sup>14</sup> and Zr-CI-based<sup>11</sup> MR fluids at pH levels of  $\sim 4$ ,  $\sim 5$ , and 6, developed in our laboratory. The initial fluid composition of the Zr-CI fluid, before the addition of any acid, is given in Table 142.V. For the experiment with the conventional fluid, each CVD ZnS substrate was spotted once for 60 s. For the experiment with the Zr-CI fluids, each substrate was spotted once at pH  $6.00 \pm 0.0$ , once at pH  $5.12 \pm 0.0$ , and once at pH  $4.22 \pm 0.1$ . Each spot lasted 10 min as a result of the lower removal rate of  $0.06$  to  $0.16 \mu\text{m}/\text{min}$  ( $0.06 \mu\text{m}/\text{min}$  at pH 4 and  $0.16 \mu\text{m}/\text{min}$  at pH 6). The Zr-CI MR fluid was first loaded on the STM at pH  $6.00 \pm 0.0$ . After spotting the substrates, the fluid pH was lowered to 5.12 using  $\sim 4$  ml of 8-M nitric acid for another round of spotting, which was followed by an additional reduction in pH to 4.22 using  $\sim 5$  ml of 8-M nitric acid. During the spotting experiment at pH 4.22, additional acid was continuously added to maintain the fluid pH level at  $\sim 4.20$ . Because of water evaporation from the MR fluids during the experiment, any addition of acid had a negligible effect on the CI particles' concentration in it. The percentage of fluid moisture when the experiment was over was 20.42%, less than 1-wt% difference from what it was at the beginning. The MR fluids at pH 4.22 will be referred to as pH 4, at 5.12 as pH 5, and at 6.00 as pH 6. The machine settings were a ribbon height of 1.4 to 1.6 mm; a penetration depth of 0.2 mm; a wheel speed of 200 rpm; a pump speed of 110 rpm; and an

Table 142.V: Initial Zr-CI MR fluid composition before adjusting pH with 8-M nitric acid. The fluid pH is  $\sim 6.0$ .

Material	$\rho$ (g/ml <sup>3</sup> )	Volume (ml)	$M$ (g)	Volume (%)	wt%
Zr-CI powder	6.72	384.80	2583.93	38.60	80.67
Polyethylenimine (PEI) solution	1.10	69.68	76.65	6.99	2.39
H <sub>2</sub> O	1.00	542.36	542.36	54.41	16.93
Total	—	996.84	3202.94	100.00	99.99

electric current of 15 Å. When the experiment was finished, each substrate had four spots on its surface, one at each pH. During the experiment, special attention was paid to removing at least 0.5  $\mu\text{m}$  at the deepest point of removal. This was based on the observations of Kozhinova *et al.*,<sup>2</sup> which stated that pebbles start to appear on pre-polished surfaces of CVD ZnS once a minimum of 0.5  $\mu\text{m}$  of material has been removed with MRF.

#### 4. MR Fluid Rheology

MR fluid off-line viscosity was measured using a Brookfield cone/plate rheometer.<sup>15</sup> At each pH, ~0.5 ml of fluid was extracted directly from the mixing vessel of the STM and placed on the viscometer plate. The fluid went through a time test in which the shear rate went from 0 1/s to 200 1/s for 30 s and then went back down to 0 1/s for another 30 s. This helped to minimize the transient behavior of the fluid. Following the time test, we measured the viscosity of the fluid as a function of shear rate from 40 to 1000 1/s. All measurements were repeated three times.

#### 5. Metrology

To evaluate the emergence of pebbles on the surface inside the spots, we used a Zygo NewView5000 white-light interferometer with a 1 $\times$  Mirau objective and a 0.8 $\times$  zoom.<sup>16</sup> The low magnification provides a large field of view that is more suitable for observing submillimeter features, such as pebbles. The spots were masked along the inner edge, and a cylinder shape was removed from the remaining masked surface. The areal rms roughness of the masked area was recorded and plotted along with ten manually drawn lineout profiles in the direction of the MRF ribbon. A power spectral density (PSD) was also analyzed in the  $x$  direction using the “average X PSD” function in the accompanying software MetroPro. To do that,

a rectangular area (2 mm  $\times$  1 mm) was masked around the depth of deepest penetration (ddp) of each spot. This analysis also provided information about the degree of waviness of the spotted surfaces.

### Results

#### 1. X-Ray Diffraction of CVD ZnS Substrates

Table 142.VI shows the XRD results of the relative intensity of crystallite orientation within the samples. For all samples, the peaks were normalized to the highest peak; i.e., for samples A, C, and D, the intensity peaks were normalized to the (111) peak, whereas for sample B, the peaks were normalized to the (311) peak. From Table 142.VI it is seen that the relative intensity rating is different among the four samples. For example, sample A's XRD results show that the (111) plane has the highest relative intensity score followed by plane (200) and then plane (311). For sample B, the ranking from high to low for the first three peaks is (311) followed by (111) and (200). This inconsistency in the order of diffracting planes is also the case for samples C and D.

#### 2. MR Fluids' Off-Line Viscosity and Material-Removal Rate

Figure 142.27 shows the off-line viscosity of all fluids as a function of shear rate. The viscosity of the Zr-CI fluid is pH dependent. It decreases as pH decreases, although the CI particle concentration has not changed (80 to 81 vol %). The fluid's off-line viscosities at ~800 (1/s)—a shear rate corresponding to that experienced by an MR fluid when ejected from the STM nozzle<sup>12</sup>—are ~60 cP for the conventional MR fluid and ~194, ~109, and ~47 cP for pH 6, 5, and 4, respectively, for the Zr-CI MR fluids. The MR fluid at pH 4 has the lowest viscosity of all fluids.

Table 142.VI: Relative intensity of CVD ZnS substrates from four vendors with respect to diffraction angle ( $2\theta$ ) and crystallographic plane. The shaded cells represent the highest peak that was used to normalize the rest of the data. FLIR: forward-looking infrared.

Approximate diffracting angle $2\theta$ ( $^\circ$ )	Diffracting planes at $2\theta$	Relative intensity within sample (%)			
		FLIR			Elemental
		Sample A JCPDS 65-0309	Sample B JCPDS 65-5476	Sample C JCPDS 65-1691	Sample D JCPDS 65-5476
28.5	111	100	70.2	100	100
33.1	200	84.3	43.8	48.0	2.14
47.5	220	25.3	15.5	23.9	22.2
56.3	311	69.3	100	59.8	13.4
59.1	222	2.1	0.9	1.6	1.7
69.5	400	48.4	28.5	33.1	1.2

Table 142.VII presents the material peak-removal rates (pr-r's) of the different fluids. The material removal rate of the Zr-CI MR fluid is significantly lower than that of the conventional MR fluid. This is expected because our MR fluids had no added abrasives, in contrast to the conventional MR fluid. However, prr results for CVD ZnS at pH 6 are similar to what were previously published by Shafrir *et al.*<sup>12</sup> when working with this type of Zr-CI particles in their MR fluid at pH 8. The Zr-CI fluid at pH 4 has the lowest prr of 0.06  $\mu\text{m}/\text{min}$ . Note that the Zr-CI MR fluid has no additive abrasives in it besides

Table 142.VII: Peak removal rate in  $\mu\text{m}/\text{min}$  of the different MR fluids and their pH level.

MR fluid type	MR fluid pH	Peak removal rate ( $\mu\text{m}/\text{min}$ )
Conventional fluid (with diamond abrasives)	10	3.50
Zr-CI (without abrasives)	6	0.16
	5	0.10
	4	0.06

possible free nanozirconia particles that are co-generated during the coating process,<sup>11,17</sup> while the conventional MR fluid contains nanodiamond abrasives.

### 3. Surface Texture and Artifacts After MRF Polishing

The surface texture inside the MRF spots is composed mostly of submillimeter features. Figure 142.28 shows the PSD (in a log scale) for CVD ZnS surfaces spotted with a conventional MR fluid at pH 10 and Zr-CI MR fluids at pH 6, 5, and 4. For all (four) vendors, results show that surface texture and waviness are higher at pH 6, somewhat lower at pH 5, but significantly lower at pH 4. When compared with the conventional MR fluid at pH 10, the use of the Zr-CI MR fluid at pH 4 is comparable. For two of the ZnS materials [Figs. 142.28(b) and 142.28(c)], the Zr-CI MR fluid leads to lower PSD than the conventional MR fluid.

The areal rms roughness and the average lineout profiles taken within the spots are presented in Figs. 142.29(a) and 142.29(b), respectively. For all vendors, when polishing with the Zr-CI MR fluids, both areal (a 2-mm  $\times$  4-mm “D”-shaped)

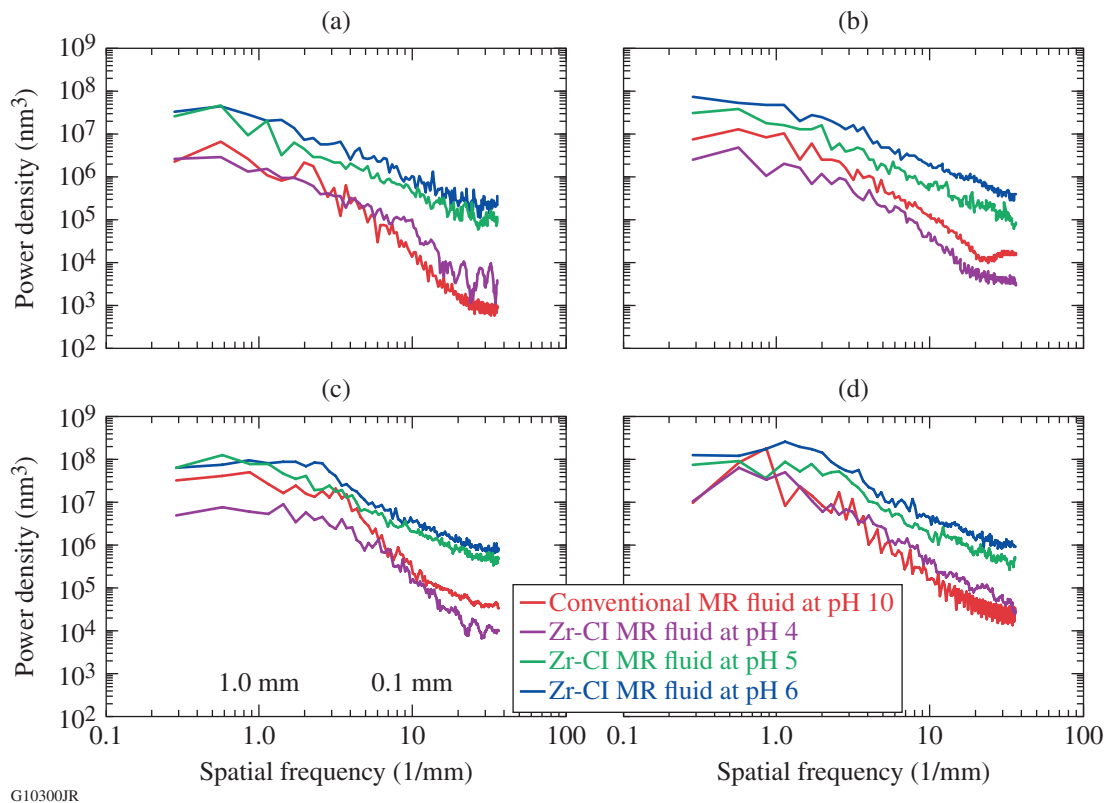
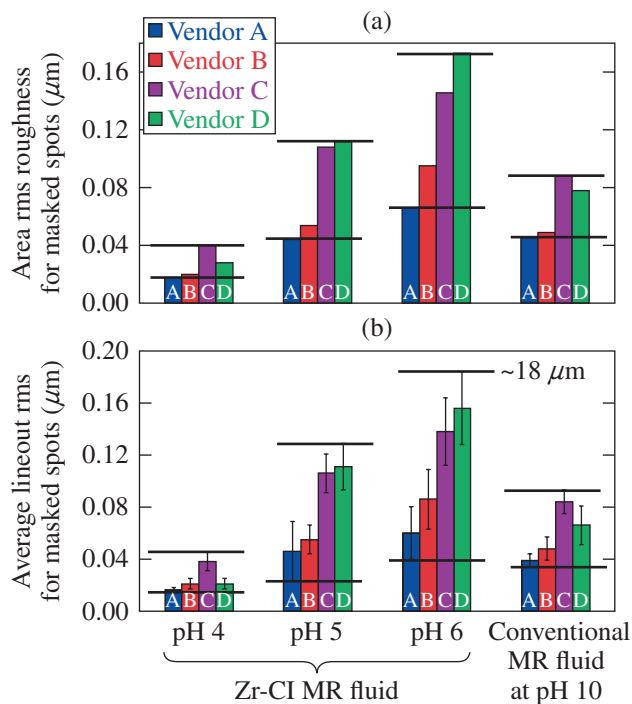


Figure 142.28 Average power spectral density (PSD) along the  $x$  direction for conventional MR fluid (blue), Zr-CI MR fluid at pH 6 (red), pH 5 (green), and pH 4 (purple) for samples A–D, respectively.



G10301JR

Figure 142.29

Macroroughness (rms) versus fluid pH for conventional MR fluid at pH 10 and Zr-CI MR fluid at pH 6, pH 5, and pH 4. (a) Areal rms roughness of a 2-mm  $\times$  4-mm “D”-shaped area; (b) average rms roughness taken from ten lineout profiles (3- to 4-mm-long lines). Horizontal lines are used to guide the eye, identifying the maximum and minimum values.

rms roughness and average lineout profiles (3 to 4 mm long) decrease with a reduction in MR fluid pH and viscosity. Moreover, the Zr-CI MR fluid at pH 4 shows lower rms roughness than the conventional MR fluid. Interestingly, variation in roughness from sample to sample is minimal when polishing with this type of fluid.

It is important to mention that roughness measurements were taken at a low resolution; therefore, it is suitable to relate to the data as it represents surface texture (at length scales 0.05 to 1 mm) rather than surface microroughness, which is not given here.

### Discussion

X-ray diffraction results for the tested substrates show that the portions of the common crystallite orientations within each sample vary from sample to sample. McCloy *et al.*<sup>18</sup> showed that the crystallographic structure and the crystallite orientations of CVD ZnS material vary along the growth direction during deposition. From their powder XRD tests, the portion of the 200 and 400 orientations in the mandrel area is higher than that in the free surface. On the contrary, the portion of the

220 orientation increases as deposition takes place. Therefore, it can be concluded that the sample crystallographic properties depend on the physical location of the cut (top, middle, or mandrel side) and the desired dimensions of the cut (thin or thick). Unless one can control the cut position when purchasing a CVD ZnS substrate, variations in the crystallographic properties are a given fact. In addition, as mentioned in the **Introduction** (p. 110), there is no consensus on deposition settings for CVD ZnS. This likely affects the relative portions of the crystallite orientations within the deposited material and adds to the variations in properties among samples purchased from different manufacturers. It is believed that this nonuniformity in crystallographic properties within the material and among materials manufactured by numerous vendors is the source for anisotropy in the material removal rate during MRF polishing, which leads to surface artifacts of CVD-grown materials, such as ZnS.

In the MRF spotting experiments, the Zr-CI MR fluids' viscosity is observed to be pH dependent. Viscosity significantly decreased with a decrease in pH because the acid increased the zeta potential of the Zr-CI particles and helped disperse the fluid as pH decreased.<sup>13</sup> The drop in viscosity also influenced the prr, which decreased consequently. The material prr of the conventional MR fluid is significantly higher than that of the Zr-CI MR fluids, even though it has relatively low viscosity. Since all fluids have similar CI particles concentration, this was likely a result of the nanodiamond abrasives within the conventional MR fluid.

From the PSD results, the MRF with Zr-CI MR fluid at pH 4 achieved a remarkable improvement in surface texture (lower spatial frequency range) and surface microroughness (higher spatial frequency range) than the fluids at pH 5 and pH 6. This is the case for all four CVD ZnS substrates. The performance of this fluid at pH 4 is slightly better than the conventional MR fluid for substrates manufactured by vendors B and C but comparable for substrates manufactured by vendors A and D. Clearly, a lower value of PSD indicates a surface with a lower texture. Therefore, it can be concluded that the emergence of pebbles on the surface of CVD ZnS substrates can be reduced when using Zr-CI MR fluid at pH 4.

Root-mean-square (rms) data collected from a masked area inside the spots and as multiple lineouts (given in Fig. 142.29) support the results obtained from PSD analysis. Reduction in surface texture is observed as the Zr-CI fluid pH and viscosity drop down. Moreover, from both areal [Fig. 142.29(a)] and lineout [Fig. 142.29(b)] results, the ability of this fluid at



pH 4 to maintain similar performances among all four tested substrates is clearly observed. Therefore, among CVD ZnS substrates deposited by different manufacturers, variations in areal and lineout rms roughness from part to part are minimal when using Zr-CI MR fluid at pH 4.

### Conclusions

It has been demonstrated that variations in the portions of crystallite orientations exist among the CVD ZnS substrates manufactured by different vendors, making it challenging to get a consistent performance during MRF polishing of such differently grown material. The results show that when several CVD ZnS substrates are polished by MRF with a Zr-CI MR fluid at pH 4, both pebble emergence and part-to-part variations in surface texture are minimized. The performance of the Zr-CI MR fluid at pH 4 was better than those of MR fluids with pH levels of 5 and 6. On the other hand, for some ZnS materials, the Zr-CI MR fluid at pH 4 produced diminished features (at a scale length of 0.03 to 1 mm) as compared to the conventional MR fluid. Of course, the Zr-CI MR fluid at low pH has a particularly low material prr, especially at pH 4, which is expected because of the absence of any abrasives. The authors believe that adding some type of abrasive, such as ceria or nanodiamonds, will likely boost the overall prr of the Zr-CI MR fluid and improve its efficiency.

### ACKNOWLEDGMENT

This material is based upon work supported by the Department of Energy National Nuclear Security Administration under Award Number DE-NA0001944, the University of Rochester, and the New York State Energy Research and Development Authority. The support of DOE does not constitute an endorsement by DOE of the views expressed in this article.

### REFERENCES

1. D. C. Harris, *Materials for Infrared Windows and Domes: Properties and Performance*, Tutorial Texts in Optical Engineering (SPIE Optical Engineering Press, Bellingham, WA, 1999), Vol. PM70.
2. I. A. Kozhinova, H. J. Romanofsky, A. Maltsev, S. D. Jacobs, W. I. Kordonski, and S. R. Gorodkin, *Appl. Opt.* **44**, 4671 (2005).
3. T. Zscheckel, W. Wisniewski, and C. Rüssel, *Adv. Funct. Mater.* **22**, 4969 (2012).
4. K. L. Lewis, A. M. Pitt, and J. A. Savage, in *Proceedings of the Ninth International Conference on Chemical Vapor Deposition 1984*, edited by Mc. D. Robinson *et al.* (Electrochemical Society, Pennington, NJ, 1984), pp. 530–545.
5. J. S. McCloy, "Properties and Processing of Chemical Vapor Deposited Zinc Sulfide," Ph.D. thesis, University of Arizona, 2008.
6. Z. Fang *et al.*, *Key Eng. Mater.* **280–283**, 537 (2005).
7. Y. Namba and H. Tsuwa, *CIRP Ann.* **28**, 425 (1979).
8. S. D. Jacobs, S. R. Arrasmith, I. A. Kozhinova, L. L. Gregg, A. B. Shorey, H. J. Romanofsky, D. Golini, W. I. Kordonski, P. Dumas, and S. Hogan, *Am. Ceram. Soc. Bull.* **78**, 42 (1999).
9. B. Hallock *et al.*, in *Frontiers in Optics 2008/Laser Science XXIV/ Plasmonics and Metamaterials/Optical Fabrication and Testing*, OSA Technical Digest (CD) (Optical Society of America, Washington, DC, 2008), Paper OThB2.
10. J. S. Goela and R. L. Taylor, *J. Mater. Sci.* **23**, 4331 (1988).
11. R. Shen, H. Yang, S. N. Shafrir, C. Miao, M. Wang, J. Mici, J. C. Lambropoulos, and S. D. Jacobs, U.S. Patent No. US 8,808,568 B2 (19 August 2014).
12. S. N. Shafrir, H. J. Romanofsky, M. Skarlinski, M. Wang, C. Miao, S. Salzman, T. Chartier, J. Mici, J. C. Lambropoulos, R. Shen, H. Yang, and S. D. Jacobs, *Appl. Opt.* **48**, 6797 (2009).
13. S. Salzman, H. J. Romanofsky, Y. I. Clara, L. J. Giannechini, G. West, J. C. Lambropoulos, and S. D. Jacobs, in *Optifab 2013*, edited by J. L. Bentley and M. Pfaff (SPIE, Bellingham, WA, 2013), Vol. 8884, Paper 888407.
14. Q22, QED Technologies, LLC, Rochester, NY 14607.
15. Brookfield DV-III Cone and Plate Viscometer, Brookfield Engineering Laboratories, Inc., Stoughton, MA 02072.
16. Zygo NewView™ 100 White Light Optical Profiler, areal over 0.25 mm × 0.35 mm with a 20× Mirau objective, no filter, Zygo Corporation, Middlefield, CT 06455.
17. R. Shen, S. N. Shafrir, C. Miao, M. Wang, J. C. Lambropoulos, S. D. Jacobs, and H. Yang, *J. Colloid Interface Sci.* **342**, 49 (2010).
18. J. McCloy, E. Fest, R. Korenstein, and W. H. Poisl, in *Window and Dome Technologies and Materials XII*, edited by R. W. Tustison (SPIE, Bellingham, WA, 2011), Vol. 8016, Paper 80160I.